# Liver Patt1 deficiency protects male mice from age-associated but not high-fat diet-induced hepatic steatosis[S]

**YangLiu,* Daizhan Zhou,* Fang Zhang,* Yanyang Tu,* Yulei Xia,* Hui Wang,* Ben Zhou,* Yi Zhang,* Jingxia Wu,* Xiang Gao,† Zhishui He,* and Qiwei Zhai[1],***

Key Laboratory of Nutrition and Metabolism, Institute for Nutritional Sciences,* Shanghai Institutes for Biological Sciences, Chinese Academy of Science; Graduate School of the Chinese Academy of Science; Shanghai 200031, China; and Model Animal Research Center,† Nanjing University, Nanjing 210061, China

**Abstract Patt1 is a newly identified protein acetyltransferase that is highly expressed in liver. However, the role of Patt1 in liver is still unclear. We generated Patt1 liver-specific knockout (LKO) mice and mainly measured the effect of hepatic Patt1 deficiency on lipid metabolism. Hepatic Patt1 deficiency in male mice markedly decreases fat mass and dramatically alleviates age-associated accumulation of lipid droplets in liver. Moreover, hepatic Patt1 abrogation in male mice significantly reduces the liver triglyceride and free fatty acid levels, but it has no effect on liver cholesterol level, liver weight, and liver function. Consistently, primary cultured Patt1-deficient hepatocytes are resistant to palmitic acid-induced lipid accumulation, but hepatic Patt1 deficiency fails to protect male mice from high-fat diet-induced hepatic steatosis. Further studies show that hepatic Patt1 deficiency decreases fatty acid uptake, reduces lipid synthesis, and enhances fatty acid oxidation, which may contribute to the attenuated hepatic steatosis in Patt1 LKO mice. These results demonstrate that Patt1 plays an important role in hepatic lipid metabolism and have implications toward resolving age-associated hepatic steatosis.**—Liu, Y., D. Zhou, F. Zhang, Y. Tu, Y. Xia, H. Wang, B. Zhou, Y. Zhang, J. Wu, X. Gao, Z. He, and Q. Zhai. **Liver Patt1 deficiency protects male mice from age-associated but not high-fat diet-induced hepatic steatosis. *J. Lipid Res.* 2012.** 53: **358–367.**

**Supplementary key words** acetyltransferase • liver-specific • lipid metabolism

Nonalcoholic fatty liver disease (NAFLD) is recognized increasingly as a major health burden (1–3). It is one of the most common causes of chronic liver disease, including cirrhosis, hepatocellular carcinoma, and liver failure. The prevalence of NAFLD increases with age, obesity, type 2 diabetes, and hypertriglyceridemia (4). Hepatic steatosis is an early stage of NAFLD, and its prevalence also increases with age, obesity, type 2 diabetes, and hyperlipidemia (5, 6). Aged mice under standard diet conditions or mice fed a high-fat diet will develop hepatic steatosis (7). Hepatic steatosis occurs as a result of excessive triglyceride accumulation in liver cells. The mechanisms of excessive hepatic triglyceride accumulation involve increased fat absorption, enhanced fat synthesis, reduced fat oxidation, and/or reduced fat export (8). However, the more detailed molecular mechanisms of hepatic steatosis need further investigation.

Many treatments for hepatic steatosis have been studied. Treatment strategies for NAFLD have revolved around identification and treatment of associated metabolic conditions such as diabetes and hyperlipidemia (9). Increasing evidence suggests that medications used for type 2 diabetes, such as metformin and thiazolidinediones, may confer a therapeutic benefit in NAFLD (10). Currently, the known effective treatment for NAFLD is modest calorie restriction and gradual weight loss (11, 12). New molecular mechanisms

*This work was supported by National Natural Science Foundation of China Grants 30825009, 30970619, 31030022 and 81021002; National Basic Research Program of China (973 Program) Grants 2009CB918403 and 2007CB914501; National Key Project of Scientific and Technical Supporting Programs Grant 2006BAI23B02; Shanghai Subject Chief Scientist Program Grant 11XD1405800, Director Foundation of the Institute for Nutritional Sciences Grant 20090101; SA-SIBS Scholarship Program; China Postdoctoral Science Foundation Grants 20100480641 and 20090450743; Shanghai Postdoctoral Scientific Program Grants 11R21417400 and 09R21416800; and Postdoctoral Fellowship Program of Shanghai Institutes for Biological Sciences, Chinese Academy of Sciences Grants 2009KIP512 and 2011KIP511.*

*Manuscript received 4 August 2011 and in revised form 27 December 2011.*

*Published, JLR Papers in Press, January 9, 2012*
*DOI 10.1194/jlr.M019257*

Abbreviations: ACC, acetyl-CoA carboxylase; ACL, ATP-citrate lyase; ACS, acyl-CoA synthetase; ALT, alanine transaminase; AST, aspartate transaminase; CPT-1, carnitine palmitoyltransferase-1; ELOVL6, elongation of long-chain fatty acids, family member 6; FATP, fatty acid transport protein; HFD, high-fat diet; LKO, liver-specific knockout; NAFLD, nonalcoholic fatty liver disease; PGC, peroxisome proliferative activated receptor γ, coactivator; PPAR, peroxisome proliferator-activated receptor; SREBP, sterol-regulatory element binding protein.

[1]To whom correspondence should be addressed.
e-mail: qwzhai@sibs.ac.cn

[S] The online version of this article (available at http://www.jlr.org) contains supplementary data in the form of 11 figures and one table.

Copyright © 2012 by the American Society for Biochemistry and Molecular Biology, Inc.



**This article is available online at http://www.jlr.org**

targeting the treatment of NAFLD need further investigation (13).

Lipid metabolism can be regulated by posttranslational modification, such as phosphorylation, ubiquitination, and acetylation (14, 15). Protein acetylation has emerged as a very important posttranslational modification in cellular metabolism regulation (16); it is a dynamic process catalyzed by deacetylases and acetyltransferases. Liver-specific deletion of SIRT1, an $NAD^+$-dependent deacetylase, impairs fatty acid oxidation and results in hepatic steatosis (17). Mice lacking SIRT3 exhibit hepatic fatty-acid oxidation disorders during fasting (18). Hepatic-specific disruption of another deacetylase SIRT6 in mice results in fatty liver formation due to enhanced glycolysis and triglyceride synthesis (19). Acetyltransferases are involved in many metabolic processes, including lipid metabolism. The p300 acetyltransferase has been reported to activate lipogenesis through histone acetylation (20). It has been reported that p300 can acetylate and stabilize sterol-regulatory element binding protein (SREBP), a key regulator in lipid metabolism (21, 22), and can acetylate peroxisome proliferator-activated receptor (PPAR)γ, which activates the transcription of multiple genes involved in lipid metabolism (23). The acetyltransferase GCN5 has been reported to acetylate peroxisome proliferative activated receptor γ, coactivator 1 β (PGC-1β) and repress the expression of its target genes involved in glucose and lipid metabolism (24). Another study reported that glucocorticoid treatment induces the acetylation of C/EBPβ by PCAF/GCN5 and thus switches on the transcription of genes involved in preadipocyte differentiation (25). Acetyltransferase PCAF has also been reported to acetylate and stabilize β-catenin (26), and the hepatic β-catenin activity affects lipid metabolism and hepatic triglyceride concentration (27). Although some acetyltransferases have been shown to be involved in the regulation of lipid metabolism, acetyltransferases involved in hepatic lipid metabolism remain to be identified.

Patt1 is a newly identified acetyltransferase belonging to the GCN5-related *N*-acetyltransferase (GNAT) family, and it is highly expressed in mouse liver (28). To investigate the role of Patt1 in liver, we used a Cre-loxP strategy to delete Patt1 specifically in liver. Our results show that liver-specific Patt1 knockout in male mice decreases fatty acid uptake, reduces lipid synthesis, enhances fatty acid oxidation, and protects mice from age-associated hepatic steatosis.

## MATERIALS AND METHODS

### Animals

All animals were maintained and used in accordance with the guidelines of the Institutional Animal Care and Use Committee of the Institute for Nutritional Sciences. C57BL/6 mice were purchased from Slac (Shanghai, China). Animals had free access to water and were fed chow with 10% kcal% fat (D12450B, Research Diets) or high-fat diet (HFD) with 45% kcal% fat (D12491, Research Diets). Mice with an albumin promoter–driven Cre transgene were obtained from Jackson Laboratory and genotyped as described by Jackson Laboratory. For HFD-induced hepatic steatosis, male mice at the age of 8 weeks were fed HFD for 14 weeks. After fasting for 6 h, animals at the indicated age were euthanized. The livers were quickly removed, snap-frozen in liquid nitrogen, and stored at −80°C for various measurements. Blood samples were obtained simultaneously for serum measurements.

### Generation of liver-specific Patt1 knockout mice

The Patt1 genomic DNA was isolated from a 129/SvJ mouse genomic library and used to construct the Patt1 targeting vector by standard techniques. The $Patt1^{+/lox}$ mice have two loxP sites inserted flanking exons 5–8 of Patt1 gene, which encode part of the Patt1 acetyltransferase domain. The $Patt1^{+/lox}$ lines from ES cells of 129/SvJ mouse strain were crossed with C57BL/6 mice for at least five generations. Then the $Patt1^{+/lox}$ mice were interbred to generate homozygous mice $Patt1^{lox/lox}$, which were crossed with the mice carrying an albumin promoter–driven Cre transgene to get the double heterozygous mice $Patt1^{+/lox}$, $Cre^{+/-}$. Subsequently, the $Patt1^{+/lox}$, $Cre^{+/-}$ mice were interbred to obtain $Patt1^{lox/lox}$, $Cre^{+/-}$ mice, and which were crossed with $Patt1^{lox/lox}$ mice to obtain sufficient Patt1 liver-specific knockout (LKO) mice $Patt1^{lox/lox}$, $Cre^{+/-}$ and littermate control mice $Patt1^{lox/lox}$ for this study. The primers for Patt1 transgenic genotyping were AATCATGGCGCCTATCAGTT and GTTTGGCTCCCTGAGTCAAG.

### Measurement of fat and lean mass, body weight, and food intake

Total body fat and lean mass of mice were measured by an NMR spectroscopy (Minispec Mq7.5; Bruker). Body weight was monitored from the age of 5 to 17 weeks, and food intake was monitored from the age of 15 to 17 weeks.

### Glucose tolerance and insulin tolerance tests

Glucose and insulin tolerance tests were performed as previously described (29). In brief, glucose tolerance tests were performed on mice fasted for 12 h, and insulin tolerance tests on mice fasted for 6 h. After fasting, the mice were injected with either 2 g/kg of glucose or 0.75 U/kg of human insulin (Lilly) into the peritoneal cavity. Blood glucose levels were measured at the indicated time points from tail blood using the FreeStyle blood glucose monitoring system (TheraSense).

### Enzyme activity measurements

Serum alanine transaminase (ALT) and aspartate transaminase (AST) were determined using enzymatic assay kits (Shensuo Unf Medical Diagnostics Articles Co., Shanghai, China).

Acetyl-CoA carboxylase (ACC) activity was measured by coupling with pyruvate kinase and lactate dehydrogenase to monitor the formation of NAD as previously described (30). Briefly, 2 μl of liver lysates at the protein concentration of 10 μg/μl were incubated with 50 μl reaction buffer containing 10 mM $NaHCO_3$, 0.4 mM NADH, 3 mM ATP, 0.4 mM acetyl-CoA, 20 U/ml pyruvate kinase (Sigma), 40 U/ml lactate dehydrogenase (Sigma), 0.5 mM phosphoenolpyruvate, 8 mM $MgCl_2$, and 100 mM HEPES at pH 8.0. The absorbance at 340 nm was monitored in a 384-well plate at 37°C for 15 min.

Carnitine palmitoyltransferase-1 (CPT-1) activity was measured by coupling to CoASH release and its reaction with 4,4'-dipyridyldisulfide as previously described (31). In brief, liver mitochondria were isolated from fresh mouse liver using a tissue mitochondria isolation kit (Beyotime Institute of Biotechnology, China). Briefly, 4 μl of the isolated liver mitochondria at the protein concentration of 5 μg/μl were incubated with 50 μl reaction

buffer containing 25 mM palmitoyl-CoA, 2 mM L-carnitine, 125 μM 4, 4'-dipyridyldisulfide, and 2 mM $KH_2PO_4$ at pH 7.5. The absorbance at 324 nm was monitored in a 384-well plate at 37°C for 15 min.

The long chain acyl-CoA synthetase (ACS) activity was also measured by coupling with pyruvate kinase and lactate dehydrogenase to monitor the formation of NAD (32). Briefly, 4 μl of liver lysates at the protein concentration of 10 μg/μl were mixed with 96 μl of the reaction mixture containing 0.5 mM oleate, 1 mM phosphoenolpyruvate, 14 mM $MgCl_2$, 1.4 mM EDTA, 0.18% Triton-X 100, 0.5 mM ATP, 2.5 mM CoA, 0.4 mM NADH, 20 U/ml myokinase, 20 U/ml pyruvate kinase, and 30 U/ml lactate dehydrogenase in a 96-well plate. The absorbance at 340 nm was monitored at 37°C for 15 min. All the hepatic enzyme activities were normalized to the respective protein concentration.

### VLDL isolation

Serum VLDL was isolated by rapid ultracentrifugation as described previously with minor modifications (33). In brief, 200 μl serum was added to a 1 ml ultracentrifuge tube, and then was gently overlaid with 100 μl of 0.196 M NaCl. Ultracentrifugation was performed in a Hitachi ultracentrifuge (CS150GX) using a fixed angle rotor (S140AT) at 140,000 rpm for 50 min at 4°C. The VLDL layer, which was located at the top of the ultracentrifuge tube, was carefully transferred to a new tube for measurement of triglyceride in VLDL.

### Measurements of triglyceride, cholesterol, and free fatty acids

Hepatic triglyceride, cholesterol, and free fatty acids were extracted as previously described (34, 35). Briefly, 40–50 mg of liver tissues or $4 \times 10^5$ cells were homogenized in 1 ml of methanol/chloroform (1:2, v/v), followed by shaking at room temperature for 2 h. Subsequently, 200 μl of 0.1 M NaCl was added, and the sample was vortexed and centrifuged at 3,000 *g* for 10 min. Then 200 μl of the organic phase was transferred to a new tube and air-dried in a fume hood overnight at room temperature. Completely dried samples were finally dissolved in 100 μl isopropanol. The triglyceride and cholesterol in serum or the samples were dissolved in isopropanol, and the triglyceride in VLDL was determined using enzymatic assay kits (Shensuo Unf Medical Diagnostics Articles Co.). The free fatty acids in serum or the samples dissolved in isopropanol were determined by a free fatty acid quantification kit (Biovision).

### Mouse primary hepatocytes isolation

Mouse primary hepatocytes were prepared from 10- to 15-week-old male mice as described previously with minor modifications (36). Male Patt1 LKO mice or their littermate controls were anesthetized, and the liver was perfused with Krebs Ringer buffer with glucose (120 mM NaCl, 4.8 mM KCl, 1.2 mM $MgSO_4$, 1.2 mM $KH_2PO_4$, 24 mM $NaHCO_3$, 20 mM glucose, and 5 mM HEPES, pH 7.45) containing 100 μM EGTA at a flow rate of 3 ml/min for 15 min. Then the perfusate was switched to Krebs Ringer buffer with glucose containing 5 mM $CaCl_2$ and 100 U/ml collagenase I (Sigma), and the perfusion was continued for another 15 min. Both perfusion buffers were prewarmed in a 37°C water bath. Subsequently, the liver was removed, minced, and dissociated in DMEM (GIBCO) on ice. The dissociated cells were then filtered through a 70 μm cell strainer and centrifuged at 50 *g* for 2 min at 4°C. Hepatocytes were washed three times with DMEM, followed by centrifugation at 50 *g* for 2 min at 4°C, and then seeded in 12-well plates precoated with mouse tail collagen (Millipore) at a concentration of $2 \times 10^5$ cells/well in DMEM with 10% FBS (GIBCO).

### Fatty acid treatment and Nile red staining

Primary hepatocytes were treated with the indicated concentrations of palmitic acid (Sigma) for 18 h, and then the primary hepatocytes were washed twice with PBS and incubated for 15 min with 2 μg/ml Nile red in PBS at 37°C. After washing twice with PBS, hepatocytes were photographed under a fluorescence microscope and then read by a microfluorometer to detect the cellular triglyceride levels as previously described (37).

### Immunoblot and immunoprecipitation

Protein samples of whole cell lysates or nuclear extracts prepared using Nuclear and Cytoplasmic Protein Extraction Kit (Beyotime, China) were analyzed with antibodies against Patt1 (28): ATP-citrate lyase (ACL), Ser79-phosphorylated ACC, ACC, FASN, C/EBPα, acetyl-lysine, and acetyl-histone H4 (Lys8) (Cell Signaling); stearoyl-Coenzyme A desaturase 1 (SCD1) and elongation of long-chain fatty acids, family member 6 (ELOVL6) (Abcam); CPT-1 (Alpha Diagnostics); SREBP1 (Santa Cruz); PGC-1β (Novus); and tubulin and actin (Sigma). The immune complexes were detected using a horseradish peroxidase-conjugated secondary antibody and visualized with a chemiluminescence reagent (Pierce). Protein quantification was performed by Quantity One software (Bio-Rad), and the intensity values were normalized to actin. Mouse liver lysates were immunoprecipitated with antibodies against SREBP1 (Santa Cruz) and PGC-1β (Novus) as described previously (26).

### Fatty acid uptake

Fatty acid uptake assay was performed as previously described (38). Briefly, primary hepatocytes in 12-well plates were incubated with 300 μl/well assay buffer (Hanks' balanced buffer containing 1% BSA and 5 μCi/ml $^3$H-palmitic acid) for 5 min at 37°C. Then the cells were washed twice with ice cold PBS and lysed with 0.3 M NaOH. The radioactivity of the cell lysates was measured by liquid scintillation counting.

### Lipid synthesis

Lipid synthesis was measured as described previously (39). Briefly, hepatocytes were incubated for 60 min at 37°C in DMEM with 10% FBS and 6 μCi/ml $^3$H-glucose. Then the hepatocytes were washed twice with PBS, and lipid was extracted as described previously (34, 35). The extracted lipid was dissolved in 1% Triton-X100, and the radioactivity of the lipid was measured by liquid scintillation counting.

### Fatty acid oxidation

Fatty acid oxidation was performed as described previously (40). Briefly, primary hepatocytes were cultured in 12-well plates for 24 h, and then washed twice with PBS. Subsequently, 300 μl assay buffer (Hanks' balanced buffer containing 10 mg/ml BSA and 3.3 μCi/ml $^3$H-palmitic acid) was added to each well and incubated at 37°C for 1 h. Then 150 μl of the assay buffer from each well was transferred to a new tube, and 400 μl methanol/chloroform (2:1, v/v) and 400 μl 2 M KCl/2 M HCl were added. After vortexing, the mixtures were centrifuged at 3,000 *g* for 5 min, and the aqueous phase containing $^3H_2O$ was transferred to a new tube to treat once more with the methanol/chloroform and KCl/HCl mixture. Finally, the aqueous phase was used to measure radioactivity.

### RNA isolation and RT-PCR

The liver total RNA was prepared using TRIzol reagent (Invitrogen) and treated with RNase-free DNase I (Takara). Then the RNA was reverse-transcribed using M-MLV Reverse Transcriptase (Promega). Real-time PCR was performed on an ABI Prism 7900

Sequence Detection System using Power SYBR Green (Applied Biosystems). The primers used for real-time PCR were mainly from PrimerBank (http://pga.mgh.harvard.edu/primerbank) and appear in supplementary Table I.

### Respiratory quotient, oxygen consumption, and total energy expenditure measurement

Respiratory quotient and oxygen consumption were determined with mice fed ad libitum using a comprehensive laboratory animal monitoring system (Columbus Instruments) according to the manufacturer's instructions. Mice were measured for 24 h after acclimation to the system for 24 h. Total energy expenditure was calculated as (3.815 + 1.232 × respiratory quotient) × $VO_2$ (41). Oxygen consumption and total energy expenditure were normalized to bodyweight or lean mass as indicated.

### Statistics

Except where indicated, data are expressed as mean ± SD of at least three independent experiments. Statistical significance was assessed by Student's *t*-test. Differences were considered statistically significant at $P < 0.05$.

## RESULTS

### Generation of liver-specific Patt1 knockout mice

The strategy to generate Patt1 liver-specific knockout (LKO) mice is shown in **Fig. 1A**. The $Patt1^{lox/lox}$, $Cre^{+/-}$ mice were crossed with $Patt1^{lox/lox}$ mice to obtain Patt1 LKO mice and littermate controls $Patt1^{lox/lox}$ mice for this study. Patt1 expression was abolished in the liver of the LKO mice compared with littermate controls (Fig. 1B), although its expression was not changed in muscle, white adipose tissue, brain, pancreas, kidney, or brown adipose tissue (Fig. 1C–E and supplementary Fig. I). These results demonstrate that the LKO mice have liver-specific deletion of Patt1.

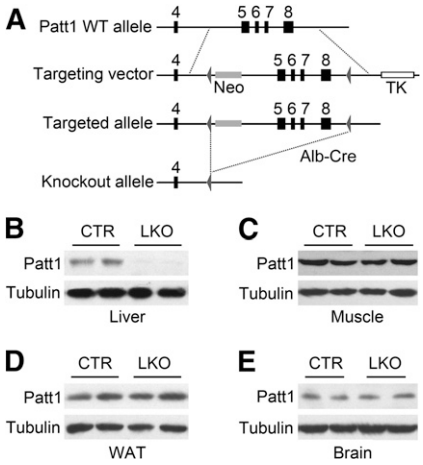


**Fig. 1.** Generation of Patt1 LKO mice. (A) Lox P sites were introduced flanking exons 5–8 of the Patt1 gene, and then exons 5–8 were deleted by crossing with mice carrying an albumin promoter–driven Cre transgene (Alb-Cre) to produce the Patt1 LKO allele. (B) Patt1 protein level markedly decreased in the liver of Patt1 LKO mice compared with littermate controls (CTR). Expression of Patt1 was measured by immunoblot, and tubulin was measured as a loading control. (C–E) Patt1 protein levels were not changed in muscle (C), white adipose tissue (WAT; D), or brain (E) as detected by immunoblot.

### Hepatic Patt1 deficiency in male mice mainly leads to markedly decreased fat mass and fat content

To evaluate the effect of liver-specific Patt1 deletion, we examined the fat and lean mass and body weight of Patt1 LKO mice. The fat mass and fat content (the ratio of fat mass to body weight) of male Patt1 LKO mice was markedly decreased at the age of 20 weeks (**Fig. 2A**, B), and even at the age of 6 or 9 weeks, a significant decrease of fat mass and fat content in male Patt1 LKO mice was observed (supplementary Fig. II). Lean mass and lean content in male Patt1 LKO mice were moderately increased at the age of 20 weeks compared with littermate controls (Fig. 2C, D). Male Patt1 LKO mice showed slightly increased body weight and food intake compared with littermate controls (Fig. 2E, F). In addition, the male Patt1 LKO mice displayed slightly improved glucose tolerance compared with littermate controls, although there was no significant difference in insulin tolerance (Fig. 2G–J). However, the female Patt1 LKO mice showed similar body weight, fat content, and lean content, and slightly increased food intake compared with littermate controls (supplementary Fig. III). Taken together, these results show that hepatic Patt1 abrogation in male mice mainly leads to markedly decreased fat mass and fat content, which suggests that Patt1 has an important role in lipid metabolism.

### Hepatic Patt1 abrogation protects against liver steatosis in male mice

We next investigated the role of Patt1 in hepatic lipid metabolism. Hematoxylin and eosin staining of liver sections showed that 31-week old male Patt1 LKO mice had much less lipid droplets in liver than littermate controls (**Fig. 3A**). Consistently, hepatic Patt1 abrogation markedly reduced the liver triglyceride content at the age of 31 weeks (Fig. 3B). Liver triglyceride content at the age of 31 weeks was significantly increased compared with that at 9 weeks in male littermate controls, but liver triglyceride content in male Patt1 LKO mice at 31 weeks was similar to that in male Patt1 LKO mice at 9 weeks (Fig. 3B). Hepatic Patt1 deficiency had no effect on liver total cholesterol level (Fig. 3C), but it significantly reduced liver free fatty acid level (Fig. 3D). Male Patt1 LKO mice had normal liver weight (Fig. 3E) and showed normal liver function when monitored by AST and ALT activities (Fig. 3F, G). Moreover, we observed elevated fasting blood glucose and declined fasting serum low-density lipoprotein cholesterol in male Patt1 LKO mice, whereas no significant changes were observed in fasting serum insulin, triglyceride, total cholesterol, high-density lipoprotein, or free fatty acid (supplementary Fig. IV). In addition, we found that mouse hepatic Patt1 protein and mRNA levels were moderately decreased at age 31 weeks compared with those levels at age 9 weeks (supplementary Fig. V, A–C), whereas Patt1 protein levels were unaffected by fasting, refeeding, and insulin treatment (supplementary Fig. V, D and E). These results demonstrate that hepatic Patt1 is associated with

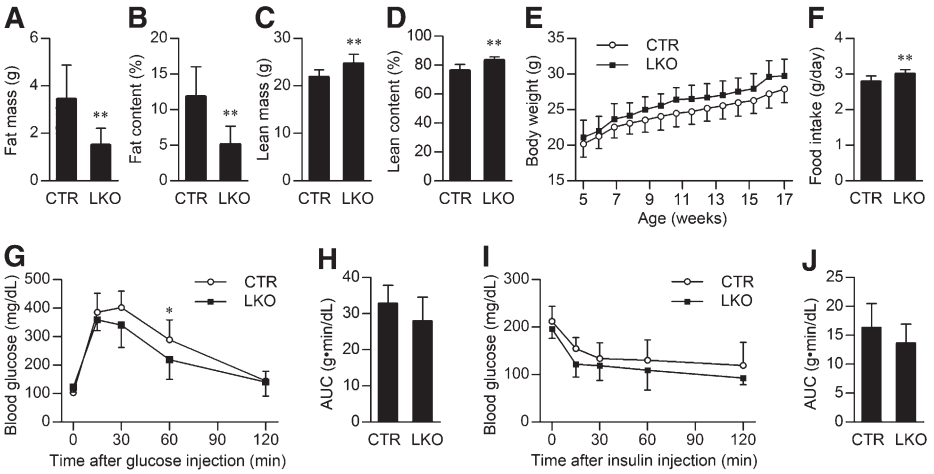


**Fig. 2.** Hepatic Patt1 deficiency mainly leads to markedly decreased fat mass and fat content. (A, B) Fat mass and fat content were markedly decreased in male Patt1 LKO mice compared with littermate controls (CTR) at the age of 20 weeks as measured by an NMR spectroscopy. (C, D) Lean mass and lean content were moderately increased in male Patt1 LKO mice at the age of 20 weeks as measured by NMR. (E) Male Patt1 LKO mice showed slightly increased bodyweight. $P = 0.0413$ as measured by two-way ANOVA. (F) Food intake of the male Patt1 LKO mice was also slightly increased at the age of 15–17 weeks. (G) Glucose tolerance was slightly improved in 15-week-old male Patt1 LKO mice as determined by glucose tolerance test. $^*P < 0.05$ versus the blood glucose level at the same time point. (H) The area under the curve (AUC) of the glucose tolerance test in (G) was similar between male Patt1 LKO mice and their littermate controls. (I) Male Patt1 LKO mice had similar insulin sensitivity as their littermate controls at the age of 17 weeks as determined by insulin tolerance test. (J) The AUC of the insulin tolerance test in (I) was similar between male Patt1 LKO mice and their littermate controls. n = 10–12/group, $^{**}P < 0.01$.

age and that its deficiency can attenuate age-associated liver steatosis in male mice.

### Hepatocytes of Patt1 LKO mice are resistant to palmitic acid–induced lipid accumulation

To further study the role of Patt1 in hepatic steatosis, we used an in vitro steatosis model induced by palmitic acid. Hepatocytes from littermate controls treated with palmitic acid developed dose-dependent accumulation of lipid droplets in cytoplasm (**Fig. 4A**), and Patt1 knockout greatly diminished the size of lipid droplets compared with the control hepatocytes (Fig. 4A). Quantification of the lipid accumulation further confirmed that Patt1 LKO hepatocytes were resistant to palmitic acid–induced lipid accumulation (Fig. 4B). The abrogation of hepatic Patt1 was confirmed by immunoblot; Patt1 protein expression was not markedly changed in control hepatocytes after treatment with palmitic acid (Fig. 4C). Consistently, intracellular triglyceride was also markedly reduced in Patt1 LKO hepatocytes (Fig. 4D). These results demonstrate that abrogation of Patt1 can effectively prevent palmitic acid-induced triglyceride accumulation in hepatocytes.

The liver steatosis mouse model induced by HFD was used for further study. After 14 weeks on a HFD, male Patt1 LKO mice showed similar fat mass, fat content, lean mass, lean content, and liver triglyceride level, and slightly increased food intake compared with littermate controls (supplementary Fig. VI, A–G). Meanwhile, hepatic Patt1 protein and mRNA levels were both dramatically downregulated in mice fed HFD compared with those levels in mice fed chow (supplementary Fig. VI, H–J). These data show that Patt1 LKO mice are not resistant to HFD-induced obesity and hepatic steatosis and that HFD dramatically reduced the expression of Patt1 in liver.

### Hepatic Patt1 knockout reduces fatty acid uptake and lipid synthesis

Hepatic steatosis could be caused by increased fatty acid uptake and upregulated lipid synthesis (42). To investigate the mechanisms of reduced liver lipid accumulation caused by hepatic Patt1 abrogation, first we checked the expression of genes related to fatty acid uptake, including CD36 and fatty acid transport protein (FATP). We found that the CD36 mRNA level decreased significantly in the liver of male Patt1 LKO mice at ages 9 and 31 weeks, whereas the FATP mRNA level was not changed (**Fig. 5A**, B). Consistently, fatty acid uptake in Patt1 knockout hepatocytes was also significantly decreased compared with control hepatocytes (Fig. 5C).

Next, we examined the expression of some key regulators involved in lipogenesis. PPARα was downregulated in 9-week-old but not in 31-week-old Patt1 LKO mice (Fig. 5D, E). It has been reported that the expression of PPARγ is markedly increased in liver of animal models with insulin resistance and fatty liver (43). As shown in Fig. 5D, E, PPARγ mRNA level decreased in the liver of male Patt1 LKO mice at ages 9 and 31 weeks, whereas the mRNA levels of C/EBPα, LXRα, and SREBP1c were not changed. Protein levels of mature SREBP1 and PGC-1β remained unchanged in the liver of male Patt1 LKO mice at ages 9 and 31 weeks (supplementary Fig. VII, A–D). Neither nuclear SREBP1 protein level nor the acetylation levels of mature SREBP1 and PGC-1β in liver were affected by hepatic Patt1 knockout (supplementary Fig. VII, E–H). It has

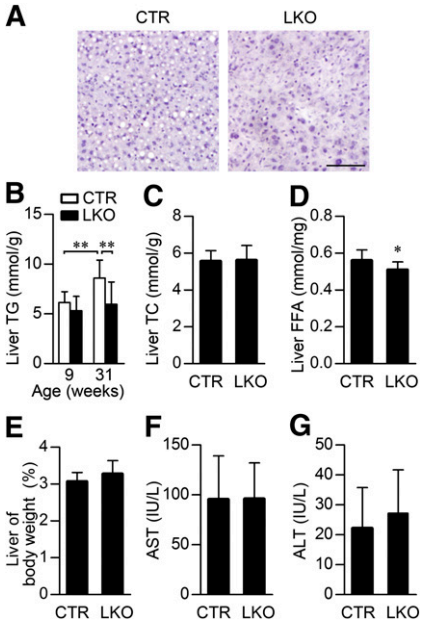


**Fig. 3.** Hepatic Patt1 abrogation protects against liver steatosis in male mice. (A) Male Patt1 LKO mice showed less lipid accumulation in liver compared with littermate controls (CTR) at the age of 31 weeks. Representative sections of the liver stained with hematoxylin and eosin are presented. Scale bar, 50 μm. (B) Hepatic Patt1 deficiency attenuated age-associated triglyceride (TG) accumulation in liver of male mice. Liver triglyceride was measured at the indicated ages. n = 8–12/group, $^{**}P < 0.01$. (C, D) Liver free fatty acid (FFA) level was attenuated in male Patt1 LKO mice at the age of 31 weeks, whereas liver total cholesterol (TC) remained at a similar level. n = 10–12/group, $^{*}P < 0.05$, $^{**}P < 0.01$. (E) The ratio of liver weight to body weight was similar between the male LKO mice and their littermate controls at the age of 31 weeks. n = 10–12/group. (F, G) Liver function of male Patt1 LKO mice was not significantly affected by liver-specific Patt1 knockout. Liver function was measured by determining serum AST and ALT levels at the age of 31 weeks. n = 10–12/group.

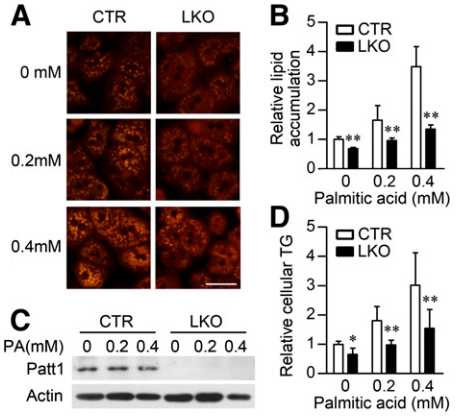


**Fig. 4.** Hepatocytes from Patt1 LKO mice are resistant to palmitic acid–induced lipid accumulation. (A) Hepatocytes from Patt1 LKO mice exhibited less lipid accumulation when challenged with the indicated concentrations of palmitic acid for 18 h. Lipid accumulation was measured by Nile red staining. Scale bar, 20 μm. (B) Quantification of the lipid accumulation in (A) was achieved by determining the red fluorescence of Nile red with a plate reader. $^{**}P < 0.01$ versus control (CTR) in the same group. (C) Patt1 protein levels in the primary mouse hepatocytes treated with the indicated concentrations of palmitic acid (PA) for 18 h were measured by immunoblot. (D) Hepatocytes from Patt1 LKO mice were resistant to PA-induced upregulation of cellular triglyceride levels. $^{*}P < 0.05$, $^{**}P < 0.01$ versus CTR in the same group.

been reported that the deacetylases SIRT1 and SIRT3 are involved in lipid metabolism (17, 18). We found that the mRNA levels of SIRT1 and SIRT3 were not changed in the liver of Patt1 LKO mice (supplementary Fig. VIII). We also tested the mRNA levels of some enzymes responsible for fatty acid and triglyceride synthesis, and we found that the mRNA level of ACL was downregulated in the liver of male Patt1 LKO mice (Fig. 5F, G). Then the protein levels of some enzymes involved in lipid synthesis were measured by immunoblot. Hepatic Patt1 deficiency downregulated the protein levels of ACL, fatty acid synthase (FAS), and ELOVL6 and upregulated the protein level of phosphorylated Ser79 ACC in liver (Fig. 5H–K). ACC catalyzes a rate-limiting step in lipid synthesis, and increased Ser79 phosphorylation of ACC has been reported leading to the inhibition of its enzyme activity (44). In agreement with that, the ACC activity in 9- and 31-week-old male Patt1 LKO mice was significantly downregulated compared with littermate controls (Fig. 5L). Consistently, lipid synthesis rates were significantly decreased in Patt1 knockout hepatocytes (Fig. 5M). Taken together, these results show that hepatic Patt1 deficiency reduces fatty acid uptake and lipid synthesis, which should contribute to the attenuated liver steatosis in male Patt1 LKO mice.

Hepatic steatosis could also be caused by decreased triglyceride export; hepatic triglyceride was exported in the form of VLDL (45). Therefore, we investigated whether hepatic Patt1 knockout could have some effect on triglyceride in VLDL. We found that serum triglyceride in VLDL was significantly downregulated in 9-week-old but not in 31-week-old male Patt1 LKO mice, indicating decreased hepatic triglyceride export in 9-week-old male Patt1 LKO mice (supplementary Fig. IX).

### Hepatic Patt1 deficiency increases fatty acid oxidation in liver

Hepatic steatosis is highly correlated with reduced lipid oxidation (8). To investigate whether Patt1 knockout had influences on fatty acid oxidation, we first assessed the protein level of CPT-1, which is the rate-limiting enzyme of fatty acid oxidation. Immunoblot analyses showed that CPT-1 protein level was significantly elevated in the liver of male Patt1 LKO mice at the age of 9 or 31 weeks (**Fig. 6A**, B). Consistently, CPT-1 enzyme activity was also significantly upregulated in the liver of male Patt1 LKO mice (Fig. 6C). Furthermore, 31-week-old male Patt1 LKO mice showed increased activity of Acyl-CoA synthetase, a crucial enzyme catalyzing the prestep reaction for β-oxidation of fatty acids, whereas no significant difference was observed in 9-week-old mice (Fig. 6D). Fatty acid oxidation assay showed that palmitic acid oxidation in Patt1 knockout hepatocytes was significantly increased compared with the control hepatocytes (Fig. 6E). Usually increased fatty acid oxidation will lead to increased ATP levels (46). As expected, hepatic ATP levels in male Patt1 LKO mice at ages 9 and 31 weeks were significantly increased (Fig. 6F).

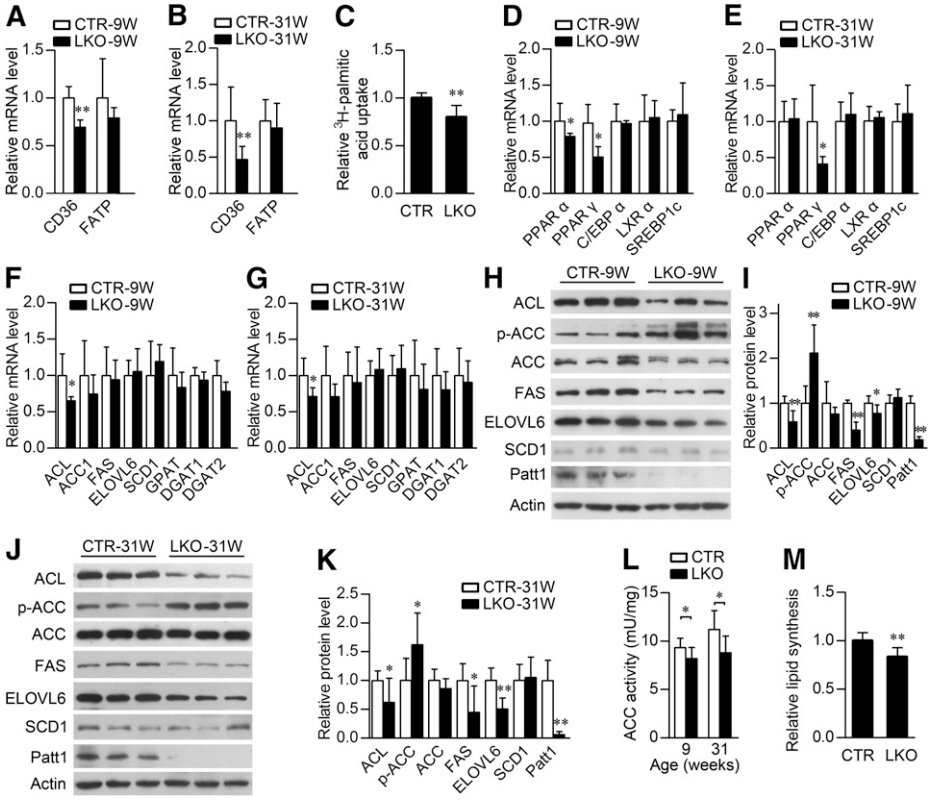


**Fig. 5.** Hepatic Patt1 knockout reduces fatty acid uptake and lipid synthesis. (A, B) Among the two indicated genes participating in fatty acid uptake, CD36 was downregulated in the liver of male Patt1 LKO mice at ages 9 weeks and 31 weeks as determined by real-time PCR. n = 4–6/group. (C) Fatty acid uptake in hepatocytes of Patt1 LKO mice was attenuated as measured by $^3$H-palmitate incorporation. Mouse primary hepatocytes were prepared from 10- to 15-week-old mice. (D, E) Among the indicated key regulators in lipid metabolism, PPARα was downregulated in 9-week-old male Patt1 LKO mice, and PPARγ was reduced in the liver of 9- and 31-week-old male Patt1 LKO mice. n = 4–6/group. (F, G) Among the indicated enzymes responsible for fatty acid and triglyceride synthesis, ACL was decreased in the liver of 9- and 31-week-old male Patt1 LKO mice. n = 4–6/group. (H, J) Among the enzymes involved in lipid synthesis, ACL, FAS, and ELOVL6 protein levels were downregulated, and the protein level of phosphorylated ACC was upregulated in the liver of 9- and 31-week-old male Patt1 LKO mice. n = 4–6/group. (I, K) Quantification of the protein levels in (H and J). (L) The activity of ACC, the rate-limiting enzyme in lipid synthesis, was attenuated in the liver of male Patt1 LKO mice. n = 8/group. (M) Lipid synthesis in hepatocytes of Patt1 LKO mice was decreased as measured by the incorporation of $^3$H-glucose into lipid. Mouse primary hepatocytes were prepared from mice at ages 10–15 weeks. $^*P < 0.05$, $^{**}P < 0.01$.

To further assess the fatty acid oxidation level at whole-body level, the respiratory quotient was measured. The male Patt1 LKO mice showed markedly decreased respiratory quotient during dark phase at the age of 22 weeks but not at the age of 9 weeks (Fig. 6G, H and supplementary Fig. X, A), suggesting decreased glycolysis and increased fatty acid oxidation in 22-week-old male Patt1 LKO mice compared with littermate controls. The 9- and 22-week-old male Patt1 LKO mice exhibited similar oxygen consumption and total energy expenditure when normalized to lean mass (Fig. 6I–L and supplementary Fig. X, B and C). However, when normalized to body weight, increased oxygen consumption and total energy expenditure during the dark phase were observed in 22-week-old but not in 9-week-old male Patt1 LKO mice (supplementary Fig. X, D and E). These results demonstrate that hepatic Patt1 deficiency enhances fatty acid oxidation in liver, which should also contribute to the attenuated liver steatosis in Patt1 LKO mice.

## DISCUSSION

Aging is associated with progressive changes in total and regional fat distribution in, for example, heart, skeletal muscle, and liver (47). Age-associated overaccumulation of fat in liver will lead to hepatic steatosis (5), but the underlying molecular mechanisms need to be further investigated. In this study, we demonstrate that hepatic Patt1 deficiency markedly attenuates age-associated hepatic steatosis (Fig. 3A, B). It is reported that there are age-related increases of fatty acid uptake and de novo lipid synthesis, and an age-related decrease of fatty acid oxidation in rat liver (48–50). Consistently, our results demonstrate that hepatic Patt1 deficiency decreases fatty acid uptake, reduces lipid synthesis, and enhances fatty acid oxidation (Figs. 5 and 6). However, female Patt1 LKO mice did not show similar phenotypes as the males (supplementary Fig. III), which might also be due to the effect of female sex

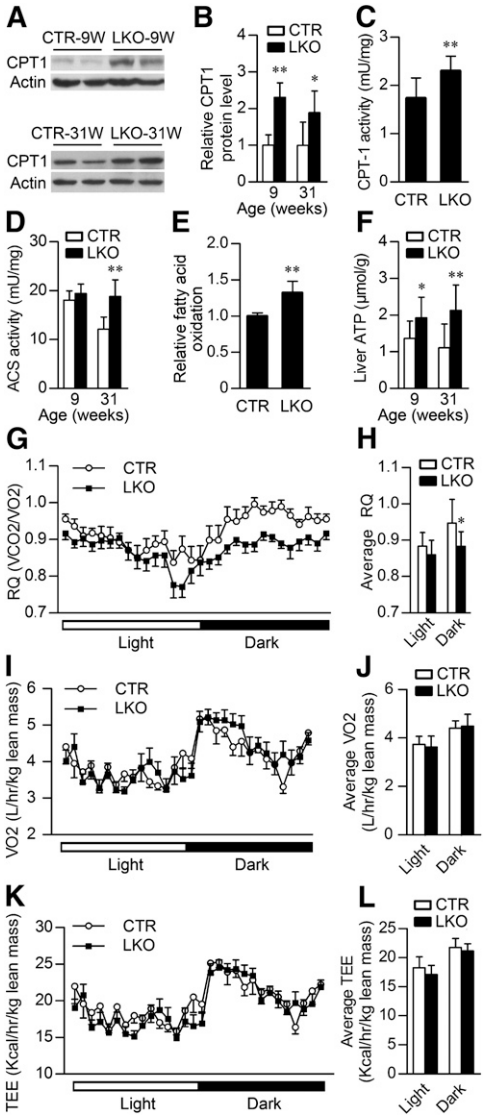


**Fig. 6.** Hepatic Patt1 deficiency increases fatty acid oxidation in liver. (A) The protein level of CPT-1, the rate-limiting enzyme in fatty acid oxidation, was upregulated in the liver of 9- and 31-week-old male Patt1 LKO mice as measured by immunoblot. (B) Quantification of CPT-1 protein levels in (A). n = 4–6/group. (C) CPT-1 activity in the liver of male Patt1 LKO mice was upregulated. n = 8. Liver mitochondria were extracted from 10-week-old male Patt1 LKO mice and littermate controls to measure CPT-1 activity. (D) The enzyme activity of ACS, a crucial enzyme catalyzing the prestep reaction for β-oxidation of fatty acids, was upregulated in the liver of 31-week-old Patt1 LKO mice compared with littermate controls. n = 8/group. (E) Fatty acid oxidation in hepatocytes of Patt1 LKO mice was increased as determined by the liberation of $^3H_2O$ from $^3$H-palmitic acid oxidation. Mouse primary hepatocytes were prepared from mice at ages 10–15 weeks. (F) At 9 and 31 weeks of age, male Patt1 LKO mice exhibited elevated hepatic ATP levels after 6 h fasting. n = 8–12/group. (G–L) At 22 weeks of age, male Patt1 LKO mice showed decreased respiratory quotient (RQ), similar oxygen consumption ($VO_2$), and total energy expenditure (TEE) at night when measured by a comprehensive laboratory animal monitoring system. n = 10/group, $^*P < 0.05$, $^{**}P < 0.01$.

hormones observed in mouse models such as diabetes and obesity (51, 52). Taken together, these results demonstrate that Patt1 knockout in liver protects male mice from age-associated increase of fatty acid uptake, upregulation of lipid synthesis, and decline of fatty acid oxidation, and it attenuates age-associated hepatic steatosis.

Although we found hepatic Patt1 deficiency decreases fatty acid uptake, reduces lipid synthesis, and enhances fatty acid oxidation in cultured hepatocytes (Figs. 5 and 6), male Patt1 LKO mice are not resistant to hepatic steatosis induced by HFD with 45% kcal% fat (supplementary Fig. VI, F). This finding suggests that although Patt1 is a modulator of hepatic lipid metabolism, it has a limited role when the liver is subjected to an increased fat load. It is very interesting that hepatic Patt1 protein and mRNA level were both dramatically downregulated in mice fed HFD to about 30% of that in mice fed chow (supplementary Fig. VI, H and I) and that hepatic Patt1 protein and mRNA levels were moderately downregulated in mice at age of 31 weeks to 60% of that in 9-week-old mice (supplementary Fig. V, A–C). When subjected to risk factors of hepatic steatosis, many genes may be actively regulated to slow down the development of steatosis. For example, it has been reported that HFD caused c-Jun N-terminal kinase (JNK) activation in liver, and hepatic JNK can prevent hepatic steatosis (53). Downregulation of Patt1 might be one of the protective responses to HFD, although hepatic Patt1 deficiency is not sufficient to attenuate the development of steatosis induced by HFD. Hepatic Patt1 protein and mRNA levels were dramatically downregulated in littermate controls fed HFD to about 30% of those in mice fed chow, and about 18% and 6% Patt1 protein were still expressed in liver of 9- and 31-week-old Patt1 LKO mice respectively compared with corresponding littermate controls (Fig. 5I, K). Because the Patt1 level in littermate controls fed HFD is close to Patt1 LKO mice, it is reasonable that Patt1 LKO had no significant effect on HFD-induced hepatic steatosis (supplementary Fig. VI, F). Future studies using mice fed HFD with less fat (e.g., with 20–35% kcal% fat) should be helpful to elucidate the potential positive effect of Patt1 LKO on hepatic steatosis induced by HFD.

In this study, we demonstrate that hepatic Patt1 deficiency influences hepatic fatty acid uptake, lipid synthesis, and fatty acid oxidation, but the underlying molecular mechanisms need further study. Histone acetyltransferase p300 has been reported to stimulate ChREBP transactivation through histone acetylation, thus to activate lipogenesis (20). Our previous study demonstrates that Patt1 locates in both nucleus and cytoplasm and exhibits histone acetyltransferase activity (28). Similarly, in this study, we found that acetylation of histone H4 (Lys8) was significantly decreased in the liver of Patt1 LKO mice (supplementary Fig. XI). So Patt1 might modulate the expression of genes involved in lipid metabolism through histone acetylation. Among the genes we have measured, CD36, PPARγ, and ACL might be modulated by Patt1 through histone acetylation, as their hepatic mRNA levels were downregulated in Patt1 LKO mice at ages 9 and 31 weeks (Fig. 5). Recent studies show that most intermediate metabolic enzymes are acetylated and that acetylation can directly affect their enzyme activity (15, 16). Furthermore, GCN5 and p300 acetylate SREBP and PGC-1β, respectively,

to regulate lipid metabolism (21, 22, 24). Although the acetylation of mature SREBP1 and PGC-1β in liver was not affected by Patt1 deficiency (supplementary Fig. VII, G and H), it is still possible that Patt1 might modulate lipid metabolism through acetylation of other proteins involved in lipid metabolism. Whether Patt1 regulates hepatic lipid metabolism through histone acetylation and/or the acetylation of proteins involved in lipid metabolism needs to be studied.

In conclusion, our study demonstrates that Patt1 LKO protects against age-associated liver steatosis in male mice, and it suggests that inhibition of hepatic Patt1 might be a potential new therapeutic strategy toward resolving hepatic steatosis.

The authors thank all members of the laboratory for sharing reagents and advice.

## REFERENCES


1. Ekstedt, M., L. E. Franzen, U. L. Mathiesen, L. Thorelius, M. Holmqvist, G. Bodemar, and S. Kechagias. 2006. Long-term follow-up of patients with NAFLD and elevated liver enzymes. *Hepatology.* **44:** 865–873.
2. Farrell, G. C., and C. Z. Larter. 2006. Nonalcoholic fatty liver disease: from steatosis to cirrhosis. *Hepatology.* **43:** S99–S112.
3. de Alwis, N. M., and C. P. Day. 2008. Non-alcoholic fatty liver disease: the mist gradually clears. *J. Hepatol.* **48(Suppl. 1):** S104–S112.
4. Bedogni, G., L. Miglioli, F. Masutti, C. Tiribelli, G. Marchesini, and S. Bellentani. 2005. Prevalence of and risk factors for nonalcoholic fatty liver disease: the Dionysos nutrition and liver study. *Hepatology.* **42:** 44–52.
5. Perez-Daga, J. A., J. Santoyo, M. A. Suarez, J. A. Fernandez-Aguilar, C. Ramirez, A. Rodriguez-Canete, J. M. Aranda, B. Sanchez-Perez, C. Montiel, D. Palomo, et al. 2006. Influence of degree of hepatic steatosis on graft function and postoperative complications of liver transplantation. *Transplant. Proc.* **38:** 2468–2470.
6. Angulo, P. 2002. Nonalcoholic fatty liver disease. *N. Engl. J. Med.* **346:** 1221–1231.
7. de Jesus, B. B., K. Schneeberger, E. Vera, A. Tejera, C. B. Harley, and M. A. Blasco. 2011. The telomerase activator TA-65 elongates short telomeres and increases health span of adult/old mice without increasing cancer incidence. *Aging Cell.* **10:** 604–621.
8. Postic, C., and J. Girard. 2008. Contribution of de novo fatty acid synthesis to hepatic steatosis and insulin resistance: lessons from genetically engineered mice. *J. Clin. Invest.* **118:** 829–838.
9. Adams, L. A., and P. Angulo. 2006. Treatment of non-alcoholic fatty liver disease. *Postgrad. Med. J.* **82:** 315–322.
10. Ahmed, M. H., and C. D. Byrne. 2009. Current treatment of non-alcoholic fatty liver disease. *Diabetes Obes. Metab.* **11:** 188–195.
11. Arendt, B. M., and J. P. Allard. 2011. Effect of atorvastatin, vitamin E and C on nonalcoholic fatty liver disease: is the combination required? *Am. J. Gastroenterol.* **106:** 78–80.
12. Ahmed, M. H., E. O. Abu, and C. D. Byrne. 2010. Non-alcoholic fatty liver disease (NAFLD): new challenge for general practitioners and important burden for health authorities? *Prim. Care Diabetes.* **4:** 129–137.
13. Musso, G., R. Gambino, and M. Cassader. 2010. Emerging molecular targets for the treatment of nonalcoholic fatty liver disease. *Annu. Rev. Med.* **61:** 375–392.
14. van Beekum, O., V. Fleskens, and E. Kalkhoven. 2009. Posttranslational modifications of PPAR-gamma: fine-tuning the metabolic master regulator. *Obesity (Silver Spring).* **17:** 213–219.
15. Guan, K. L., and Y. Xiong. 2011. Regulation of intermediary metabolism by protein acetylation. *Trends Biochem. Sci.* **36:** 108–116.
16. Zhao, S., W. Xu, W. Jiang, W. Yu, Y. Lin, T. Zhang, J. Yao, L. Zhou, Y. Zeng, H. Li, et al. 2010. Regulation of cellular metabolism by protein lysine acetylation. *Science.* **327:** 1000–1004.
17. Purushotham, A., T. T. Schug, Q. Xu, S. Surapureddi, X. Guo, and X. Li. 2009. Hepatocyte-specific deletion of SIRT1 alters fatty acid metabolism and results in hepatic steatosis and inflammation. *Cell Metab.* **9:** 327–338.
18. Hirschey, M. D., T. Shimazu, E. Goetzman, E. Jing, B. Schwer, D. B. Lombard, C. A. Grueter, C. Harris, S. Biddinger, O. R. Ilkayeva, et al. 2010. SIRT3 regulates mitochondrial fatty-acid oxidation by reversible enzyme deacetylation. *Nature.* **464:** 121–125.
19. Kim, H. S., C. Xiao, R. H. Wang, T. Lahusen, X. Xu, A. Vassilopoulos, G. Vazquez-Ortiz, W. I. Jeong, O. Park, S. H. Ki, et al. 2010. Hepatic-specific disruption of SIRT6 in mice results in fatty liver formation due to enhanced glycolysis and triglyceride synthesis. *Cell Metab.* **12:** 224–236.
20. Bricambert, J., J. Miranda, F. Benhamed, J. Girard, C. Postic, and R. Dentin. 2010. Salt-inducible kinase 2 links transcriptional coactivator p300 phosphorylation to the prevention of ChREBP-dependent hepatic steatosis in mice. *J. Clin. Invest.* **120:** 4316–4331.
21. Giandomenico, V., M. Simonsson, E. Gronroos, and J. Ericsson. 2003. Coactivator-dependent acetylation stabilizes members of the SREBP family of transcription factors. *Mol. Cell. Biol.* **23:** 2587–2599.
22. You, M., X. Liang, J. M. Ajmo, and G. C. Ness. 2008. Involvement of mammalian sirtuin 1 in the action of ethanol in the liver. *Am. J. Physiol. Gastrointest. Liver Physiol.* **294:** G892–G898.
23. Gelman, L., G. Zhou, L. Fajas, E. Raspe, J. C. Fruchart, and J. Auwerx. 1999. p300 interacts with the N- and C-terminal part of PPARgamma2 in a ligand-independent and -dependent manner, respectively. *J. Biol. Chem.* **274:** 7681–7688.
24. Kelly, T. J., C. Lerin, W. Haas, S. P. Gygi, and P. Puigserver. 2009. GCN5-mediated transcriptional control of the metabolic coactivator PGC-1beta through lysine acetylation. *J. Biol. Chem.* **284:** 19945–19952.
25. Wiper-Bergeron, N., H. A. Salem, J. J. Tomlinson, D. Wu, and R. J. Hache. 2007. Glucocorticoid-stimulated preadipocyte differentiation is mediated through acetylation of C/EBPbeta by GCN5. *Proc. Natl. Acad. Sci. USA.* **104:** 2703–2708.
26. Ge, X., Q. Jin, F. Zhang, T. Yan, and Q. Zhai. 2009. PCAF acetylates {beta}-catenin and improves its stability. *Mol. Biol. Cell.* **20:** 419–427.
27. Liu, H., M. M. Fergusson, J. J. Wu, I. I. Rovira, J. Liu, O. Gavrilova, T. Lu, J. Bao, D. Han, M. N. Sack, et al. 2011. Wnt signaling regulates hepatic metabolism. *Sci. Signal.* **4:** ra6.
28. Liu, Z., Y. Liu, H. Wang, X. Ge, Q. Jin, G. Ding, Y. Hu, B. Zhou, Z. Chen, B. Zhang, et al. 2009. Patt1, a novel protein acetyltransferase that is highly expressed in liver and downregulated in hepatocellular carcinoma, enhances apoptosis of hepatoma cells. *Int. J. Biochem. Cell Biol.* **41:** 2528–2537.
29. Sun, C., F. Zhang, X. Ge, T. Yan, X. Chen, X. Shi, and Q. Zhai. 2007. SIRT1 improves insulin sensitivity under insulin-resistant conditions by repressing PTP1B. *Cell Metab.* **6:** 307–319.
30. Blanchard, C. Z., Y. M. Lee, P. A. Frantom, and G. L. Waldrop. 1999. Mutations at four active site residues of biotin carboxylase abolish substrate-induced synergism by biotin. *Biochemistry.* **38:** 3393–3400.
31. Ramsay, R. R., J. P. Derrick, A. S. Friend, and P. K. Tubbs. 1987. Purification and properties of the soluble carnitine palmitoyltransferase from bovine liver mitochondria. *Biochem. J.* **244:** 271–278.
32. Kasuya, F., K. Igarashi, and M. Fukui. 1996. Participation of a medium chain acyl-CoA synthetase in glycine conjugation of the benzoic acid derivatives with the electron-donating groups. *Biochem. Pharmacol.* **51:** 805–809.
33. McEneny, J., C. McMaster, E. R. Trimble, and I. S. Young. 2002. Rapid isolation of VLDL subfractions: assessment of composition and susceptibility to copper-mediated oxidation. *J. Lipid Res.* **43:** 824–831.
34. Chung, C., J. A. Doll, A. K. Gattu, C. Shugrue, M. Cornwell, P. Fitchev, and S. E. Crawford. 2008. Anti-angiogenic pigment epithelium-derived factor regulates hepatocyte triglyceride content through adipose triglyceride lipase (ATGL). *J. Hepatol.* **48:** 471–478.
35. Wang, Q., L. Jiang, J. Wang, S. Li, Y. Yu, J. You, R. Zeng, X. Gao, L. Rui, W. Li, et al. 2009. Abrogation of hepatic ATP-citrate lyase protects against fatty liver and ameliorates hyperglycemia in leptin receptor-deficient mice. *Hepatology.* **49:** 1166–1175.
36. Mathijs, K., A. S. Kienhuis, K. J. Brauers, D. G. Jennen, A. Lahoz, J. C. Kleinjans, and J. H. van Delft. 2009. Assessing the metabolic

competence of sandwich-cultured mouse primary hepatocytes. *Drug Metab. Dispos.* **37:** 1305–1311.
37. Donato, M. T., A. Lahoz, N. Jimenez, G. Perez, A. Serralta, J. Mir, J. V. Castell, and M. J. Gomez-Lechon. 2006. Potential impact of steatosis on cytochrome P450 enzymes of human hepatocytes isolated from fatty liver grafts. *Drug Metab. Dispos.* **34:** 1556–1562.
38. Park, S. G., Y. S. Kang, J. Y. Kim, C. S. Lee, Y. G. Ko, W. J. Lee, K. U. Lee, Y. I. Yeom, and S. Kim. 2006. Hormonal activity of AIMP1/p43 for glucose homeostasis. *Proc. Natl. Acad. Sci. USA.* **103:** 14913–14918.
39. Joost, H. G., and H. J. Steinfelder. 1982. Modulation of insulin sensitivity by adenosine. Effects on glucose transport, lipid synthesis, and insulin receptors of the adipocyte. *Mol. Pharmacol.* **22:** 614–618.
40. Abu-Elheiga, L., W. Oh, P. Kordari, and S. J. Wakil. 2003. Acetyl-CoA carboxylase 2 mutant mice are protected against obesity and diabetes induced by high-fat/high-carbohydrate diets. *Proc. Natl. Acad. Sci. USA.* **100:** 10207–10212.
41. Sleeman, M. W., K. Garcia, R. Liu, J. D. Murray, L. Malinova, M. Moncrieffe, G. D. Yancopoulos, and S. J. Wiegand. 2003. Ciliary neurotrophic factor improves diabetic parameters and hepatic steatosis and increases basal metabolic rate in db/db mice. *Proc. Natl. Acad. Sci. USA.* **100:** 14297–14302.
42. Musso, G., R. Gambino, and M. Cassader. 2009. Recent insights into hepatic lipid metabolism in non-alcoholic fatty liver disease (NAFLD). *Prog. Lipid Res.* **48:** 1–26.
43. Browning, J. D., and J. D. Horton. 2004. Molecular mediators of hepatic steatosis and liver injury. *J. Clin. Invest.* **114:** 147–152.
44. Ha, J., S. Daniel, S. S. Broyles, and K. H. Kim. 1994. Critical phosphorylation sites for acetyl-CoA carboxylase activity. *J. Biol. Chem.* **269:** 22162–22168.
45. Hooper, A. J., L. A. Adams, and J. R. Burnett. 2011. Genetic determinants of hepatic steatosis in man. *J. Lipid Res.* **52:** 593–617.
46. Orellana-Gavaldà, J. M., L. Herrero, M. I. Malandrino, A. Paneda, M. Sol Rodriguez-Pena, H. Petry, G. Asins, S. Van Deventer, F. G. Hegardt, and D. Serra. 2011. Molecular therapy for obesity and diabetes based on a long-term increase in hepatic fatty-acid oxidation. *Hepatology.* **53:** 821–832.
47. Kuk, J. L., T. J. Saunders, L. E. Davidson, and R. Ross. 2009. Age-related changes in total and regional fat distribution. *Ageing Res. Rev.* **8:** 339–348.
48. Tollet-Egnell, P., P. Parini, N. Stahlberg, I. Lonnstedt, N. H. Lee, M. Rudling, A. Flores-Morales, and G. Norstedt. 2004. Growth hormone-mediated alteration of fuel metabolism in the aged rat as determined from transcript profiles. *Physiol. Genomics.* **16:** 261–267.
49. Murthy, V. K., O. A. Oredipe, M. R. Stiles, and J. C. Shipp. 1986. Increased fatty acid uptake, a factor in increased hepatic triacylglycerol synthesis in aging rats. *Mech. Ageing Dev.* **37:** 49–54.
50. Mori, S., N. Morisaki, Y. Saito, and S. Yoshida. 1988. Age-related changes of long-chain fatty acid metabolism in rat liver. *Mech. Ageing Dev.* **44:** 175–183.
51. Church, C., S. Lee, E. A. Bagg, J. S. McTaggart, R. Deacon, T. Gerken, A. Lee, L. Moir, J. Mecinovic, M. M. Quwailid, et al. 2009. A mouse model for the metabolic effects of the human fat mass and obesity associated FTO gene. *PLoS Genet.* **5:** e1000599.
52. Wang, S., N. Yehya, E. E. Schadt, H. Wang, T. A. Drake, and A. J. Lusis. 2006. Genetic and genomic analysis of a fat mass trait with complex inheritance reveals marked sex specificity. *PLoS Genet.* **2:** e15.
53. Sabio, G., J. Cavanagh-Kyros, H. J. Ko, D. Y. Jung, S. Gray, J. Y. Jun, T. Barrett, A. Mora, J. K. Kim, and R. J. Davis. 2009. Prevention of steatosis by hepatic JNK1. *Cell Metab.* **10:** 491–498.